Spatial variations of a passive tracer in a random wave field

Roman E. Glazman[1] and Peter B. Weichman[2]
[1]Jet Propulsion Laboratory 300-323G, California Institute of Technology, Pasadena, CA 91109
[2]Blackhawk Geometrics, 301 Commercial Rd., Suite B, Golden, CO 80121

Abstract

The effect of random wave fields on passive tracer spatial variations is studied. We derive a closed form expression for the spatial autocorrelation function (or power spectrum) of the tracer fluctuations that is quantitatively accurate so long as wave field nonlinearities are small. The theory is illustrated for the case of long internal gravity waves in the ocean. We find that even if the spectrum of the advecting velocity field is a pure power law, the tracer spectum has two separate power law subranges. Most important to oceanographic applications, in the larger scale region the effective horizontal compressibility of the wave velocity field becomes a dominant factor of the tracer variations. In such cases, the concentration spectrum becomes approximately proportional to the spectrum of the wave potential energy. The latter, which decays with increasing wavenumber much more rapidly than that known for two-dimensional eddy turbulence, is confirmed by satellite observations in wave-dominated ocean regions.

1 Introduction

Spatial variations of sea surface temperature, chlorophyll concentration and other tracers reflect, among other factors, a pattern of water motions in the upper ocean layer. In the range of scales from 10^0-10^2 kilometers, oceanic motions are essentially two-dimensional and their kinetic energy spectrum $E(k)$, according to theoretical predictions for two-dimensional eddy turbulence, is controlled by the direct inertial cascade of enstrophy: $E(k) = C_\Omega \epsilon_\Omega^{2/3} k^{-3}$, where ϵ_Ω is the rate of enstrophy transfer in the spectral cascade and C_Ω is a universal constant. Present theory of turbulent transport then predicts the wavenumber spectrum of a spatially-varying field of tracer concentration to be proportional to k^{-1} (see, e.g., [1, 2, 3]). Many observations, however, yield much higher rates of spectral roll-off (see, e.g., [4, 5, 6] and references therein) – as fast as k^{-3} – in the range $1 \lesssim 2\pi/k \lesssim 100$km. While various explanations have been suggested for these higher rates (see, e.g., [7]), none of them questioned the 2-D eddy turbulence as an important dynamical factor of tracer dispersion on these short scales.

In the present work we study fluctuations originating from a different source of oceanic motions, namely those caused by random *waves*. While the formal theory presented here is general, the results will be specialized and applied in the end to the case of baroclinic inertia gravity (BIG) waves, since these waves represent one of two major classes of large-scale oceanic motions. The theory of passive tracer fluctuations in random wave fields presented in this paper should lead to better understanding of the observed patterns of tracer field concentration, including patchiness of biological fields.

As will be shown in Sec. 3, in certain areas of the ocean BIG waves dominate the kinematics of the passive tracer field, at least on scales $1 \lesssim 2\pi/k \lesssim 100$km. Such areas include many high-latitude regions in which eddy turbulence tends to be generally weak. In general, the kinetic energy of eddy turbulence in the world ocean (excepting, of course, the strong ocean current areas such as the Gulf Stream or the Antarctic Circumpolar Current region) rapidly decreases with an increasing latitude [9]. It is well known ([8]) (and has been confirmed by numerical models of ocean dynamics [9]) that the characteristic size of ocean eddies generated by baroclnic instability of ocean shear flows is comparable to the local Rossby radius of deformation. At high latitudes, the baroclinic Rossby radius is under 20km. The energy of vortical turbulence is transferred from this range to larger scales through the inverse Kolmogorov-type spectral cascade, and the velocity spectrum behaves approximately as $k^{-5/3}$. The spectrum of BIG wave turbulence in the inverse cascade range behaves as k^{-3} ([10]), and therefore grows at a more rapid rate as k decreases. Thus, if the energy of both the vortical and the wave motions is generated at high wavenumbers, the relative intensity of eddy turbulence at wavenumbers below the generation range (i.e, on scales greater than, say, 20km) could drop well below that of BIG wave turbulence. Spatial variations of tracer fields may thus be affected by wave motions in a rather broad spectral range. The passive tracer spectrum measured by Gower et al. (1980) [4] at 60°N latitude (where the Rossby radius is below 10 km), reproduced in Fig. 1, confirms this theory. This will be discussed in more detail and supported with more recent experimental data in Sec. 3.

Passive scalar dynamics is governed by the transport equation

$$\partial_t q + \nabla \cdot (\mathbf{v} q) = 0 \tag{1}$$

for the concentration field $q(\mathbf{x}, t)$ advected by a random wave velocity field $\mathbf{v}(\mathbf{x}, t)$, which in this work will be taken to be spatially-homogeneous and statistically stationary. Molecular diffusion, which is generally extremely small on the scale of turbulent diffusion, is neglected. It is commonly assumed that $\mathbf{v}$ is incompressible, $\nabla \cdot \mathbf{v} = 0$, but for wave fields, where one is interested mainly in horizontal transport, one is led naturally to effective *two-dimensional* descriptions – such as the shallow water equations – where the variation of the height of the free surface, or of isopycnal surfaces, leads to an effectively *compressible* horizontal velocity field $\mathbf{v}$. This property will turn out to be crucial to the strong influence of the wave field on the passive tracer concentration field: the compressional part of the wave field leads directly to fluctuations in the tracer concentration. In all that follows all vectors will be restricted to the horizontal plane.

We will derive a closed-form solution for the autocorrelation function

$$R(\mathbf{x}-\mathbf{x}') = \langle q(\mathbf{x},t)q(\mathbf{x}',t)\rangle, \tag{2}$$

in which the average is over the appropriate ensemble of wave fields determined by the statistics of $\mathbf{v}$. In contrast to the classical problem of particle dispersion by eddy turbulence (reviewed, e.g., in Chapter 5 of [12] and, more recently, in [13]) where no small parameter exists, wave-induced dispersion can be treated in a rigorous, controlled mathematical fashion [14, 15]. The derivation is based on the short-correlation approximation (reviewed, for example, in [16]) which, in the case of wave turbulence, is well justified: the time scale of typical wave oscillation periods (which is of the same order as the autocorrelation timescale for the fluctuating field $q(\mathbf{x},t)$) is much shorter than the timescale on which the evolution of $\langle q(\mathbf{x},t)\rangle$, $\langle q(\mathbf{x}_1,t)q(\mathbf{x}_2,t)\rangle$, etc. is observed.

We find also that even if the advecting velocity field has a pure power law turbulent spectrum, there emerge two separate power law subranges in the tracer spectrum. It is found that at larger scales a linearized version of the passive tracer transport equation is valid, and leads to a power-law dominated by the compressive part of the velocity field. However, at smaller scales, essentially nonlinear effects dominate, and a different power-law obtains.

The closed-form expression for $R(\mathbf{r})$ obtained in this work is rather general and applies to either linear or nonlinear waves of an arbitrary nature – provided only that their nonlinearity is sufficiently weak. Conversely, the wave-induced diffusion studied in [14, 15] is a second-order effect, associated with the wave nonlinearity, and vanishes for purely linear waves. Thus, the present effect is much stronger and easier to observe.

2 Theory of tracer fluctuations

2.1 Quick derivation

In order to understand, at the simplest possible level, the direct relationship between passive scalar statistics and statistics of the velocity field $\mathbf{v}$, consider the limit in which $\mathbf{v}$ is small. Let $\bar{q}$ be the overall mean tracer concentration, and assume that the fluctuating part $q(\mathbf{x}) - \bar{q}$ is also small. This is actually an independent assumption since the size of the latter is set by initial conditions and may be large even if the former is small. The latter assumption will be lifted in the formal derivation in the next subsection. Linearizing (1) one obtains

$$\partial_t q = -\bar{q}\nabla\cdot\mathbf{v} \tag{3}$$

In most cases the full three-dimensional field is incompressible, so one is assuming here a projected description in which only the horizontal velocity components are taken into account, and q has been vertically integrated. Such a description may be rigorously derived [15], but we shall not discuss this procedure further here. From (3) it immediately follows that

$$\begin{aligned}\Delta R(\mathbf{x}-\mathbf{x}',t) &\equiv \langle[q(\mathbf{x},t)-q_0(\mathbf{x})][q(\mathbf{x}',t)-q_0(\mathbf{x}')]\rangle \\ &= \bar{q}^2\int_0^t ds_1\int_0^t ds_2\langle\nabla\cdot\mathbf{v}(\mathbf{x},s_1)\nabla'\cdot\mathbf{v}(\mathbf{x}',s_2)\rangle \\ &= -\bar{q}^2\sum_{i,j}\partial_i\partial_j\int_0^t ds_1\int_0^t ds_2 G_{ij}(\mathbf{x}-\mathbf{x}',s_1-s_2), \end{aligned} \tag{4}$$

in which $q_0(\mathbf{x}) = q(\mathbf{x},0)$ is the initial concentration field, the average is over the ensemble of velocity fields $\mathbf{v}$, and

$$G_{ij}(\mathbf{x}-\mathbf{x}',t-t') = \langle v_i(\mathbf{x},t)v_j(\mathbf{x}',t')\rangle \tag{5}$$

is the velocity correlator. Noting that for any function $f(t)$ that decays to zero rapidly for $|t| > \tau$, where τ is the decorrelation time of the wave field,

$$\begin{aligned}\int_0^t ds\int_0^t ds' f(s-s') &= \int_{-t}^t ds(t-|s|)f(s) \\ &\to t\hat{f}(0) - \int_{-\infty}^{\infty} ds|s|f(s), \end{aligned} \tag{6}$$

where $\hat{f}(\omega)$ is the Fourier transform of $f(t)$ and the last line follows for $|t| > \tau$, one obtains

$$\Delta R(\mathbf{r},t) \to \bar{q}^2\sum_{i,j}\partial_i\partial_j\left[-t\hat{G}_{ij}(\mathbf{r},\omega=0) + \int_{-\infty}^{\infty} ds|s|G_{ij}(\mathbf{r},s)\right]. \tag{7}$$

The term linear in t represents diffusive decorrelation – the coefficient $D_{ij} = \frac{1}{2}\hat{S}_{ij}(0)$, where $\hat{S}_{ij}(\omega) = \hat{G}_{ij}(\mathbf{0},\omega)$ is the frequency spectrum, in fact represents the lowest order result for the wave-induced diffusion tensor [15]. Now, for wave fields it transpires that $\hat{G}_{ij}(\mathbf{r}',\omega)$ vanishes in a neighborhood of $\omega = 0$: for BIG waves the dispersion relation has a gap about $\omega = 0$ given by the Coriolis parameter f, while for other types of waves $\omega = 0$ corresponds to waves of infinite wavelength which do not exist in the ocean. The term linear in t therefore vanishes to lowest order and, after a transient of duration τ, the autocorrelation kernel relaxes to the time independent form given by the second term in (7). Converting the time integral to a frequency integral, this may be expressed in the form

$$\Delta R(\mathbf{r}) = -\bar{q}^2\sum_{i,j}\partial_i\partial_j\int\frac{d\omega}{2\pi\omega^2}\hat{G}_{ij}(\mathbf{r},\omega), \tag{8}$$

and its spatial Fourier transform is

$$\Delta\hat{R}(\mathbf{k}) = \bar{q}^2\sum_{i,j}\int\frac{d\omega}{2\pi}\frac{k_ik_j}{\omega^2}\Phi_{ij}(\mathbf{k},\omega), \tag{9}$$

In which $\hat{\Phi}_{ij}(\mathbf{k},\omega)$ is the full spatio-temporal Fourier transform of $G_{ij}(\mathbf{r},t)$. Now, for wave fields $\hat{\Phi}_{ij}$ is nonzero only on surfaces determined by the wave dispersion relation $\omega(\mathbf{k})$:

$$\Phi_{ij}(\mathbf{k},\omega) = F_{ij}(\mathbf{k})2\pi\delta[\omega-\omega(\mathbf{k})] + F_{ji}(-\mathbf{k})2\pi\delta[\omega+\omega(-\mathbf{k})], \tag{10}$$

in which $F_{ij}(\mathbf{k})$ is the wavenumber spectrum. One therefore obtains finally the simple result

$$\Delta\hat{R}(\mathbf{k}) = \bar{q}^2 k^2 \left[\frac{F_L(\mathbf{k})}{\omega(\mathbf{k})^2} + \frac{F_L(-\mathbf{k})}{\omega(-\mathbf{k})^2}\right], \tag{11}$$

where $F_L(\mathbf{k}) = \sum_{i,j} \hat{k}_i \hat{k}_j F_{ij}(\mathbf{k})$ is the longitudinal (compressional) part of the wavenumber spectrum. The fact that only F_L enters is obvious in retrospect since the divergences imply that only the longitudinal part of $\mathbf{v}$ enters (4), and this exhibits the direct connection between the compressive nature of $\mathbf{v}$ and fluctuations in the tracer concentration. For an isotropic spectrum and dispersion relation, (11) reduces to

$$\Delta\hat{R}(\mathbf{k}) = 2\bar{q}^2 \frac{k^2 F_L(k)}{\omega(k)^2}. \tag{12}$$

Notice that (4) implies that the wave spectrum alters the tracer spectrum ***additively.*** Thus suppose that at time $t = 0$ there exists a "background" spectrum $\hat{R}_0(\mathbf{k})$ obtained from the spatial Fourier transform of

$$R_0(\mathbf{x} - \mathbf{x}') = [q_0(\mathbf{x}) q_0(\mathbf{x}')]_{\mathrm{av}}, \tag{13}$$

in which, for the purposes of this calculation, we assume that the initial condition $q_0(\mathbf{x})$ is characteristic of transport processes *excluding* BIG waves. The initial condition is therefore stochastic in character and $[\cdot]_{\mathrm{av}}$ then denotes an appropriate ensemble average. For a large enough statistically homogeneous region A, an equivalent operational definition is

$$R_0(\mathbf{r}) = \int \frac{d^d x}{A} q_0(\mathbf{x} + \mathbf{r}) q_0(\mathbf{x}), \tag{14}$$

in which the dimension is $d = 2$ for most applications, but we keep d general for computational convenience and generality. A full theory, which is beyond the scope of this work, would have to account simultaneously for the effects of the (possibly interacting) vortical eddy and wave field modes. We may suppose, however that vortical motions are slow on the scale of a typical BIG wave period, and hence that we may ignore further vortical motions while we consider the evolution of q on such time scales. One sees from the above calculation that after a time of order the wave field decorrelation time τ, that the full observed spectrum $\hat{R}(\mathbf{k})$, obtained from the Fourier transform of

$$R(\mathbf{x} - \mathbf{x}') = \langle [q(\mathbf{x}, t) q(\mathbf{x}', t)]_{\mathrm{av}} \rangle, \tag{15}$$

"equilibrates" to a new steady state, given by the sum

$$\hat{R}(\mathbf{k}) = R_0(\mathbf{k}) + \Delta\hat{R}(\mathbf{k}), \tag{16}$$

that incorporates the spectrum of the BIG wave field. However, the additive nature of this spectral renormalization means, in particular, that observation of the effects of waves on passive tracer fluctuations in any particular part of the spectrum requires that the wave energy spectrum be of the same order or larger than the eddy energy spectrum. If such is the case, this then provides a possible explanation for the more rapid than expected fall-off in the observed spectrum of concentration field fluctuations: see Sec. 3 below for a more detailed discussion.

2.2 Formal theory

In order to confirm the content of (13) and (16) we turn to a full theory of passive tracer fluctuations. This will allow us to evaluate the range of validity of the quick derivation and to understand the origin of any corrections. The results derived in this subsection will be valid for an initial $q_0(\mathbf{x})$ with arbitrarily large fluctuations, so long as $\mathbf{v}$ is at most weakly nonlinear.

The formal theory [15] is based on a Lagrangian representation of the passive scalar distribution. Let $\mathbf{Z}_{\mathbf{x}t}(s)$ be the (Lagrangian) position of a fluid particle at time s, provided this particle has been (or will be) found at point $\mathbf{x}$ at time t. As shown in [15], the tracer concentration field may then be represented in the form

$$q(\mathbf{x},t) = \int d^dx' q_0(\mathbf{x}')\delta[\mathbf{x} - \mathbf{Z}_{\mathbf{x}'0}(t)] = q_0[\mathbf{Z}_{\mathbf{x}t}(0)]\det[\partial\mathbf{Z}_{\mathbf{x}t}(0)/\partial\mathbf{x}], \tag{17}$$

where $q_0(\mathbf{x}) = q(\mathbf{x}, t = 0)$ is the initial concentration field, and the Jacobian determinantal factor accounts for the "compressibility" of the horizontal velocity field $\mathbf{v}$ in the horizontal plane $\mathbf{x}$, i.e., for the fact that $\nabla \cdot \mathbf{v} \neq 0$.

The calculation proceeds as follows. Using the random walk representation, the double-ensemble averaged equal-time autocorrelation function is given by

$$\begin{aligned} R(\mathbf{x}-\mathbf{x}',t) &= \langle [q(\mathbf{x},t)q(\mathbf{x}',t)]_{\mathrm{av}}\rangle \\ &= \int d^dy \int d^dy' [q_0(\mathbf{y})q_0(\mathbf{y}')]_{\mathrm{av}} \langle \delta[\mathbf{x} - \mathbf{Z}_{\mathbf{y}0}(t)]\delta[\mathbf{x}' - \mathbf{Z}_{\mathbf{y}'0}(t)]\rangle \\ &= \int \frac{d^dk}{(2\pi)^d} \int \frac{d^dk'}{(2\pi)^d} \int d^dy \int d^dy' R_0(\mathbf{y}-\mathbf{y}') e^{i\mathbf{k}\cdot(\mathbf{x}-\mathbf{y})+i\mathbf{k}'\cdot(\mathbf{x}'-\mathbf{y}')} e^{-\lambda(\mathbf{k},\mathbf{k}';\mathbf{y}-\mathbf{y}',t)}, \end{aligned} \tag{18}$$

where in the last line the Fourier representation of the delta-functions has been used and, letting $\Delta\mathbf{Z}_{\mathbf{y}0}(t) \equiv \mathbf{Z}_{\mathbf{y}0}(t) - \mathbf{y}$, we define the characteristic functional

$$\lambda(\mathbf{k},\mathbf{k}';\mathbf{y}-\mathbf{y}',t) \equiv -\ln\langle e^{-i\mathbf{k}\cdot\Delta\mathbf{Z}_{\mathbf{y}0}(t) - i\mathbf{k}'\cdot\Delta\mathbf{Z}_{\mathbf{y}'0}(t)}\rangle. \tag{19}$$

Changing variables to $\mathbf{r}' = \mathbf{y}-\mathbf{y}'$ and $\mathbf{Y} = (\mathbf{y}+\mathbf{y}')/2$, we see that the only dependence of the integrand in (18) on the center of mass variable $\mathbf{Y}$ is through an exponential factor $\exp i(\mathbf{k}+\mathbf{k}')\cdot\mathbf{Y}$. The $\mathbf{Y}$-integration therefore produces a delta function enforcing $\mathbf{k}+\mathbf{k}' = \mathbf{0}$. One obtains then

$$R(\mathbf{r}) = \int d^dr' R_0(\mathbf{r}')\mathcal{K}(\mathbf{r},\mathbf{r}',t), \tag{20}$$

in which the integration kernel $\mathcal{K}$ is given by

$$\mathcal{K}(\mathbf{r},\mathbf{r}',t)=\int\frac{d^dk}{(2\pi)^d}e^{i\mathbf{k}\cdot(\mathbf{r}-\mathbf{r}')-\lambda(\mathbf{k},-\mathbf{k};\mathbf{r}',t)}. \tag{21}$$

Noting that $\hat{R}_0(\mathbf{k})=(2\pi)^d\bar{q}^2\delta(\mathbf{k})+\tilde{R}_0(\mathbf{k})$ and $\hat{R}(\mathbf{k})=(2\pi)^d\bar{q}^2\delta(\mathbf{k})+\tilde{R}(\mathbf{k})$ contain delta-function pieces coming from the fact that their real space forms asymptote to $\bar{q}^2$ for large r, in Fourier space one obtains the equivalent form

$$\tilde{R}(\mathbf{k})=\bar{q}^2\hat{\mathcal{K}}(\mathbf{k},\mathbf{0},t)+e^{-\lambda_\infty(\mathbf{k},-\mathbf{k},t)}\tilde{R}_0(\mathbf{k})+\int\frac{d^dk'}{(2\pi)^d}\hat{\mathcal{K}}(\mathbf{k},\mathbf{k}',t)\tilde{R}_0(\mathbf{k}') \tag{22}$$

in which $\hat{\mathcal{K}}$ is given by

$$\hat{\mathcal{K}}(\mathbf{k},\mathbf{k}',t)=\int d^dr'e^{-i(\mathbf{k}-\mathbf{k}')\cdot\mathbf{r}'}\left[e^{-\lambda(\mathbf{k},-\mathbf{k};\mathbf{r}',t)}-e^{-\lambda_\infty(\mathbf{k},-\mathbf{k};t)}\right]. \tag{23}$$

The subtraction

$$\begin{aligned}e^{-\lambda_\infty(\mathbf{k},-\mathbf{k},t)} &= \lim_{|\mathbf{r}'|\to\infty} e^{-\lambda_\infty(\mathbf{k},-\mathbf{k};\mathbf{r}',t)}\\ &= |\langle e^{-i\mathbf{k}\cdot\Delta\mathbf{Z}_{\mathbf{y}0}(t)}\rangle|^2\end{aligned} \tag{24}$$

is required to eliminate the corresponding delta-function terms in $\hat{\mathcal{K}}$ itself. We will see that the quick result of the previous subsection emerges in an appropriate limit from the first two terms in (22).

To evaluate $\mathcal{K}$ more explicitly an approximate scheme for computing λ must be developed. As shown in [15], for wave fields there exists a well defined perturbation theory in the small parameter u_0/c_0, where $u_0=\sqrt{\langle\mathbf{v}^2\rangle}$ is the typical particle velocity and c_0 is the typical phase speed of the waves. Under typical ocean conditions one finds $u_0/c_0=O(10^{-1})$. The perturbation theory is implemented first by performing a cummulant expansion in powers of $\Delta\mathbf{Z}$:

$$\begin{aligned}\lambda(\mathbf{k},-\mathbf{k};\mathbf{y}-\mathbf{y}',t) &= i\cdot\langle\mathbf{k}\cdot[\Delta\mathbf{Z}_{\mathbf{y}0}(t)-\Delta\mathbf{Z}_{\mathbf{y}0}(t)]\rangle\\ &+ \frac{1}{2}\langle\{\mathbf{k}\cdot[\Delta\mathbf{Z}_{\mathbf{y}0}(t)-\Delta\mathbf{Z}_{\mathbf{y}0}(t)]\}^2\rangle_c+O[(ku_0t)^3],\end{aligned} \tag{25}$$

in which the subscript c indicates that the product of the averages should be subtracted. The first term represents the mean relative drift of two particles a distance $\mathbf{r}'$ apart. Since we are considering a homogeneous situation, so that $\langle\Delta\mathbf{Z}_{\mathbf{y}0}(t)\rangle$ is independent of $\mathbf{y}$, this term vanishes identically. Defining the Lagrangian correlator

$$\Gamma_{ij}(\mathbf{y}-\mathbf{y}',t)=\langle[\Delta\mathbf{Z}_{\mathbf{y}0}(t)-\Delta\mathbf{Z}_{\mathbf{y}'0}(t)]_i[\Delta\mathbf{Z}_{\mathbf{y}0}(t)-\Delta\mathbf{Z}_{\mathbf{y}'0}(t)]_j\rangle \tag{26}$$

and neglecting all higher order terms in λ (which is valid for small $ku_0\tau$, i.e., on length scales larger than the typical distance travelled by a tracer particle in a typical wave period – roughly a factor u_0/c_0

times the dominant wavelength), we obtain then

$$\begin{aligned}
\mathcal{K}(\mathbf{r},\mathbf{r}',t) &= \int \frac{d^dk}{(2\pi)^2} e^{i\mathbf{k}\cdot(\mathbf{r}-\mathbf{r}')} e^{-\frac{1}{2}\sum_{i,j}\Gamma_{ij}(\mathbf{r}',t)k_ik_j} \\
&= \frac{e^{-\frac{1}{2}\sum_{i,j}\Gamma_{ij}^{-1}(\mathbf{r}',t)(\mathbf{r}'-\mathbf{r})_i(\mathbf{r}'-\mathbf{r})_j}}{\sqrt{\det[2\pi\Gamma(\mathbf{r}',t)]}},
\end{aligned} \tag{27}$$

in which Γ_{ij}^{-1} is the inverse of the matrix Γ_{ij}. The kernel $\mathcal{K}$ therefore reflects explicitly the Lagrangian autocorrelations. The theory presented in [15] now also allows one to evaluate Γ_{ij} perturbatively in terms of Eulerian velocity correlators of the wave field. First, one has the exact defining relation

$$\Delta\mathbf{Z}_{\mathbf{y}0}(t) = \int_0^t ds\mathbf{v}(\mathbf{Z}_{\mathbf{y}0}(s),s). \tag{28}$$

Second, if $\Delta\mathbf{Z}_{\mathbf{y}0}(t) = O(u_0t)$ is small compared to the typical length scale of variation of $\mathbf{v}(\mathbf{y},t)$ (given by the typical wavelength $\lambda_0 = c_0t_0$, where t_0 is the wave period), i.e., if u_0t/c_0t_0 is small (which will be the case if t is not too much larger than t_0 – we will see below that we only need t up to the decorrelation time τ, which is indeed typically of the same order as t_0) one may simply replace $\mathbf{v}(\mathbf{Z}_{\mathbf{y},0}(s),s)$ by its Eulerian counterpart $\mathbf{v}(\mathbf{y},t)$, with corrections of relative order u_0/c_0 (which may be computed in a gradient expansion of $\mathbf{v}$ [15]). Thus, in terms of the Eulerian velocity correlator (5), one obtains to lowest order

$$\Gamma_{ij}(\mathbf{r},t) = \int_0^t ds \int_0^t ds'[2G_{ij}(\mathbf{0},s-s') - G_{ij}(\mathbf{r},s-s') - G_{ij}(-\mathbf{r},s-s')], \tag{29}$$

with corrections of relative $O(u_0^2/c_0^2)$. Using (6) one obtains

$$\Gamma_{ij}(\mathbf{r},t) \to t[\hat{G}_{ij}(\mathbf{0},0) - \hat{G}_{ij}(\mathbf{r},0)] - \int_{-\infty}^{\infty} ds|s|[G_{ij}(\mathbf{0},s) - G_{ij}(\mathbf{r},s)] + (i \leftrightarrow j), \quad t > \tau. \tag{30}$$

The term linear in t once again vanishes for wave turbulence, and after a transient of duration τ, the autocorrelation kernel relaxes to the time independent form

$$\mathcal{K}_\infty(\mathbf{r},\mathbf{r}') \equiv \mathcal{K}(\mathbf{r},\mathbf{r}',\infty) = \frac{e^{-\frac{1}{2}\sum_{i,j}\gamma_{ij}^{-1}(\mathbf{r}')(\mathbf{r}'-\mathbf{r})_i(\mathbf{r}'-\mathbf{r})_j}}{\sqrt{\det[2\pi\gamma(\mathbf{r}',t)]}} \tag{31}$$

$$\hat{\mathcal{K}}_\infty(\mathbf{k},\mathbf{k}') = \int d^dr' e^{-i(\mathbf{k}-\mathbf{k}')\cdot\mathbf{r}'}\left[e^{-\frac{1}{2}\sum_{i,j}\gamma_{ij}(\mathbf{r}')k_ik_j} - e^{-\frac{1}{2}\sum_{i,j}\gamma_{ij}(\infty)k_ik_j}\right], \tag{32}$$

with

$$\begin{aligned}
\gamma_{ij}(\mathbf{r}) &= -\int_{-\infty}^{\infty} ds|s|[G_{ij}(\mathbf{0},s) - G_{ij}(\mathbf{r},s)] + (i \leftrightarrow j) \\
&= \int_{-\infty}^{\infty} \frac{d\omega}{2\pi\omega^2}[\hat{S}_{ij}(\omega) - \hat{G}_{ij}(\mathbf{r},\omega)] + (i \leftrightarrow j) \\
&= 2\int \frac{d^dk}{(2\pi)^d}\frac{F_{ij}(\mathbf{k}) + F_{ji}(\mathbf{k})}{\omega(\mathbf{k})^2}[1 - \cos(\mathbf{k}\cdot\mathbf{r})].
\end{aligned} \tag{33}$$

and therefore

$$\begin{aligned}\gamma_{ij}(\infty) &= \int_{-\infty}^{\infty} \frac{d\omega}{2\pi\omega^2}[\hat{S}_{ij}(\omega) + \hat{S}_{ji}(\omega)] \\ &= 2\int \frac{d^d k}{(2\pi)^d} \frac{F_{ij}(\mathbf{k}) + F_{ji}(\mathbf{k})}{\omega(\mathbf{k})^2}. \end{aligned} \tag{34}$$

The Fourier transform of $\tilde{\gamma}_{ij}(\mathbf{r}) \equiv \gamma_{ij}(\infty) - \gamma_{ij}(\mathbf{r})$ is then

$$\tilde{\gamma}_{ij}(\mathbf{k}) = \left[\frac{F_{ij}(\mathbf{k}) + F_{ji}(\mathbf{k})}{\omega(\mathbf{k})^2} + \frac{F_{ij}(-\mathbf{k}) + F_{ji}(-\mathbf{k})}{\omega(-\mathbf{k})^2}\right] \tag{35}$$

Higher order corrections actually produce a linear time dependence with corrected diffusion coefficient of relative $O(u_0^2/c_0^2)$ [15] which then produces diffusive decorrelation on a much larger time scale of $O(c_0^2\tau/u_0^2)$.

2.3 Calculation of spectral renormalization

The effect of the kernel $\mathcal{K}$ on the background autocorrelation function $\hat{R}_0(\mathbf{k})$ depends crucially on the range of k that one is considering. The result (32) is valid so long as k^2 times the leading [relative $O(u_0^2/c_0^2)$] corrections to (29) are small, i.e., if $k^2u_0^4\tau^2/c_0^2 \sim (k\lambda_0)^2(u_0/c_0)^4 << 1$, where $\lambda_0 \sim c_0t_0$ is a characteristic length determined by the spectral peak frequency. Thus k should be small compared to $c_0^2/u_0^2\lambda_0 \sim c_0/u_0d_0$, where $d_0 = u_0t_0$ is the typical distance travelled by the tracer particle in a dominant wave period. Since c_0^2/u_0^2 is typically of order 10^2, this puts the upper bound on allowed k nearly two decades into the inertial range of $\mathbf{v}$. Due to the complexity of the relations (20) and (22), however, the inertial range power law spectra of $\mathbf{v}$ do *not* lead immediately in the same range to simple power law spectra for q. Rather, as we now demonstrate, although the inertial range behavior of $\mathbf{v}$ determines that of q, different spectral power laws for q are exhibited in different ranges of k.

Let us first rederive (16). Suppose that k is sufficiently small that $k^2\gamma_{ij}(\mathbf{r})$ is small, i.e., $k^2(u_0\tau)^2 \sim (k\lambda_0)^2(u_0/c_0)^2 \ll 1$. This requires then that k be small compared to $c_0/u_0\lambda_0 \sim 1/d_0$, limiting it to less than a decade into the inertial range. One may then expand $\hat{\mathcal{K}}_\infty(\mathbf{k},\mathbf{k}')$ in the form

$$\begin{aligned}\hat{\mathcal{K}}_\infty(\mathbf{k},\mathbf{k}') &= \int d^d r' e^{-i(\mathbf{k}-\mathbf{k}')\cdot\mathbf{r}'}\left[\frac{1}{2}\sum_{i,j}\tilde{\gamma}_{ij}(\mathbf{r}')k_ik_j + O[(u_0\tau k)^4]\right] \\ &= \frac{1}{2}\sum_{i,j}\tilde{\gamma}_{ij}(\mathbf{k}-\mathbf{k}')k_ik_j[1 + O(u_0^2\tau^2k^2)]. \end{aligned} \tag{36}$$

Inserting this into (22), the first term reduces precisely to (11) and one obtains (16), but now with leading corrections:

$$\tilde{R}(\mathbf{k}) = \Big\{\hat{R}_0(\mathbf{k}) + \Delta\hat{R}(\mathbf{k})$$

$$- \frac{1}{2}R_0(\mathbf{k})\sum_{i,j} k_i k_j \left[\gamma_{ij}(\infty)\tilde{R}_0(\mathbf{k}) - \int \frac{d^d k'}{(2\pi)^d}\tilde{\gamma}_{ij}(\mathbf{k}-\mathbf{k}')\tilde{R}_0(\mathbf{k}')\right]\Bigg\}[1+O(k^2u_0^2\tau^2)]. \tag{37}$$

The original quick derivation was based on the assumption that fluctuations in q were small compared to the mean $\bar{q}$, i.e., that $\tilde{R}_0(\mathbf{k}) \ll \bar{q}^2$. Under this condition the second line of (37) is small compared to the first two terms, and (16) is rigorously recovered.

We remark in passing that the k-space approximation used in (36) may also be implemented in the real space version form (31). The small k limit is equivalent to the limit where r is sufficiently large that $\gamma_{ij}(\mathbf{r}')$ is slowly varying over the range of $\mathbf{r}'$ for which the exponential numerator in (31) is not vanishingly small, i.e., the limit where the replacement of $\gamma_{ij}(\mathbf{r}')$ by $\gamma_{ij}(\mathbf{r})$ in the exponential is permitted. The real space form of (37) is then obtained by making this replacement and then performing a second order Taylor expansion of the determinant denominator of the right hand side of (31) in the difference $\mathbf{r}'-\mathbf{r}$.

Suppose next that $1/d_0 \le k \ll c_0/u_0d_0$, so that the Taylor expansion of the exponential is no longer appropriate. In the real space form this means that $\mathbf{r}$ is small enough that $\gamma_{ij}(\mathbf{r}')$ is varying substantially over the range where the exponential numerator in (31) is nonvanishing. The analysis in this regime is most simply carried out directly in real space. To simplify the calculations we will consider only the case where the spectrum of $\mathbf{v}$ is isotropic, and $\gamma_{ij}(\mathbf{r}) = \gamma(r)\delta_{ij}$ is diagonal. Isotropy actually allows a more general form with independent longitudinal and transverse components, $\gamma_L(r)$ and $\gamma_T(r)$, but we treat here only the simplest case $\gamma_T = \gamma_L$. One obtains then

$$\mathcal{K}_\infty(r', |\mathbf{r}'-\mathbf{r}|) = \frac{e^{-|\mathbf{r}'-\mathbf{r}|^2/2\gamma(r')}}{[2\pi\gamma(r')]^{d/2}}. \tag{38}$$

Since $\gamma(r')$ vanishes as $r' \to 0$ this kernel becomes a delta-function in $\mathbf{r}$ at this point. For r' away from the origin, $\mathcal{K}$ roughly averages $R_0(r')$ over an area of radius $\sqrt{\gamma}$. The behaviour of the Fourier spectrum $\hat{R}_0(k)$ at large k reflects itself in the behavior of $R_0(r)$ at small r. Thus, if the spectrum decays rapidly, $R_0(r)$ will have a Taylor expansion in r^2 about the origin. If the spectrum decays as a slow power law, $k^{-(d+\alpha)}$ (with dimension $d=2$ in the present case), then one will have a leading behavior of the form $R_0(r) = R_0(0)[1-Ar^\alpha]$ (with $\alpha<0$ permitted). Similarly, if the BIG wave spectrum decays as a slow power law, one will have the leading behavior $\gamma(r) = Br^\beta$ with, typically, $0<\beta<2$.

Given the two exponents α and β, the final question we address is the resulting leading behavior $R(r) = R(0)[1-Cr^\mu]$. In particular, what is the function $\mu(\alpha,\beta)$? This function can be inferred from the analysis of the integral (48) in the Appendix A with the identification $\sigma = -\alpha - d(2-\beta)/2$. In addition to analytic contributions to $R(r)$, there is a leading nonanalytic contribution with exponent

$$\mu(\alpha,\beta) = -2\sigma/\beta = 2(\alpha+d)/\beta - d. \tag{39}$$

This exponent then translates into a large k Fourier space (angular integrated) spectral form $\sim k^{-p}$ with

$$p(\alpha,\beta) = \mu(\alpha,\beta) + d - (d-1) = 2(\alpha+d)/\beta + 1 - d. \tag{40}$$

3 Discussion and conclusions

Equations (16) and (39) are the basic results of this paper. One sees that even if the initial concentration field correlator $R_0(r)$ is analytic [corresponding to rapid decay of $\tilde{R}_0(k)$ for large k], indicating a smooth initial condition, these equations will produce nontrivial power law behavior in $\hat{R}(k)$. Considering first the range $k\lambda_0 < c_0/u_0$ where (16) is valid, if $F(k) \approx F_0 k^{-d-q}$ and $\omega(k) \approx C_0 k^{\zeta}$ in this range, then the angle integrated tracer spectrum will vary as

$$k^{d-1}\Delta\hat{R}(k) \sim k^{1-q-2\zeta}, \quad k\lambda_0 < c_0/u_0. \tag{41}$$

For BIG waves, Now, as alluded to in the Introduction, the (angle integrated) BIG wave wavenumber spectrum $k^{d-1}F(k)$ (with $d=2$) is observed to vary as $k^{-4/3}$ for $ck \gg f$. This corresponds to $F(k) \sim k^{-7/3}$, and hence $q = 1/3$. In this range one has simply $\omega(k) \approx ck$, i.e., $\zeta = 1$, and we obtain then $k^{d-1}\Delta\hat{R}(k) \sim k^{-p}$, with $p = 4/3$. This result assumes that the direct energy cascade dominates. However, BIG waves also have an inverse cascade of *wave action* that yields $k^{d-1}F(k) \sim k^{-3}$, corresponding to $q = 2$ and hence $k^{d-1}\Delta\hat{R}(k) \sim k^{-p}$ with $p = 3$. Since the wavenumber range over which most of the external energy/action input occurs is not known, the precise wavenumber separating the direct and inverse cascades is not known. Both theory and observations [11] seem to indicate that k^{-3} behavior may extend to length scales as short as 20km, with $k^{-4/3}$ behavior observable only on yet shorter scales. It is therefore possible that it is precisely under these circumstances that k^{-3} tracer spectra are being observed. Clearly, depending upon the precise ocean conditions, and hence the exact balance between the various terms entering the determination of $\hat{R}(k)$, the present theory allows an effective tracer spectral exponent anywhere within the observed range $1 \le p \le 3$.

Consider next the range $c_0/u_0 < \lambda_0 k < (c_0/u_0)^2$ in which (39) is valid. This equation will produce a series of singularities corresponding to non-negative even integer values of α. The leading singularity (corresponding to $\alpha = 0$) takes the form (in $d = 2$),

$$\mu(0,\beta) = 4/\beta - 2, \quad p(0,\beta) = 4/\beta - 1 \tag{42}$$

corresponding to a Fourier space spectral decay $k^{-(d+\mu)} = k^{-4/\beta}$. Interestingly, the more fractal like is the wave velocity field spectrum (the smaller the value of β), the less fractal like is (the steeper is the fall off of) the passive tracer spectrum. The $1/k$ theoretical (angular integrated) spectrum alluded to in the introduction corresponds to the case of a logarithmic divergence in $R_0(r)$ as $r \to 0$. This yields, effectively, $\alpha = 0$ and (42) is predicted to be valid, up to possible logarithmic corrections. A value $\beta = 1$ would then produce a wave-field renormalized k^{-3} spectrum, consistent with observations.

Let us now derive a form for β for a given behavior of the frequency or wavenumber spectrum. The full wavenumber-frequency spectrum for a general wave field is given by (10) in which the dispersion relation is $\omega(\mathbf{k}) = \sqrt{f^2 + c^2k^2}$ for BIG waves, where $f = 2\Omega\sin(\phi)$ is the Coriolis parameter (Ω begin the earth's rotation frequency and ϕ being the latitude). In the isotropic approximation in which we work, we assume $F_{ij}(\mathbf{k}) = \frac{1}{d}F(k)\delta_{ij}$ and consider only isotropic $\omega(\mathbf{k}) = \omega(k)$ so that the total kinetic energy spectrum (the trace of Φ_{ij}) is

$$\Phi(k,\omega) = 2\pi F(k)\{\delta[\omega - \omega(k)] + \delta[\omega + \omega(k)]\}. \tag{43}$$

¿From (38) and (56) one then obtains

$$\begin{aligned}\gamma(r) &= \frac{2}{d}\int \frac{d^dk}{(2\pi)^d}\int \frac{d\omega}{2\pi\omega^2}\Phi(k,\omega)\left[1 - e^{i\mathbf{k}\cdot\mathbf{r}}\right] \\ &= \frac{4}{d}\int \frac{d^dk}{(2\pi)^d}\frac{F(k)}{\omega(k)^2}\left[1 - e^{i\mathbf{k}\cdot\mathbf{r}}\right]\end{aligned} \tag{44}$$

Thus, if $F(k) \approx F_0 k^{-d-q}$ and $\omega(k) \approx C_0 k^\zeta$ for large k, $\gamma(r)$ will have a singular term varying as

$$\gamma_{\text{sing}}(r) = \gamma_s r^{q+2\zeta}, \quad \gamma_s = \frac{2^{2-q-2\zeta}F_0}{d(4\pi)^{d/2}C_0^2}\frac{\Gamma\left(-\zeta - \frac{q}{2}\right)}{\Gamma\left(\zeta + \frac{d+q}{2}\right)}, \tag{45}$$

in which (56) and relation 6.561.14 (p. 684) of [17] has been used.

If $q + 2\zeta < 2$ then this will be the leading term, and one immediately identifies $\beta = q + 2\zeta$. On the other hand, if $q + 2\zeta > 2$ then this singular term will be subleading, and $\gamma(r)$ will have a leading r^2 term given by

$$\gamma(r) = \gamma_2 r^2 + \gamma_s r^{q+2\zeta} + O(r^4), \quad \gamma_2 = \frac{4}{d^2}\int \frac{d^dk}{(2\pi)^d}\frac{k^2F(k)}{\omega(k)^2}. \tag{46}$$

In this case one would then identify $\beta = 2$, and one then infers the general relation,

$$\beta = \min\{q + 2\zeta, 2\}. \tag{47}$$

For $q > 0$ and $\zeta = 1$ one has $2\zeta + q > 2$ and we infer that $\beta = 2$ in all the cases discussed above. The results in the Appendix A [case (vi)] then imply that $\mu = \alpha$: the initial spectrum is unrenormalized in this range of larger k.

We conclude that the effects of BIG waves on the passive tracer spectrum are expected to be strongest only in the smaller k range where (12) and (16) are valid. For BIG waves the spectral peak is at the Coriolis frequency f. The characteristic length $\lambda_0 \sim c/f \equiv R$ is then determined by the Rossby radius R.

At mid-latitudes $R \sim$ 20-40km. The condition for the validity of (12) and (16) is then that $k < c_0/u_0 R$, i.e., that length scales $\lambda > 2\pi(u_0/c_0)R \sim$ 10-20km be considered.

For BIG waves, one has the relation $k^2 F_L(k)/\omega(k)^2 = (\rho_* c^2)^{-1} U(k)$, where ρ_* is the average water density and $U(k)$ is the potential spectrum (which can be inferred from satellite altimeter data). In Fig. 2 we display an example of such a $U(k)$, showing the k^{-3} behavior discussed above. This theoretical spectrum has been confirmed by satellite altimeter observations of sea surface height variations on scales from about 70km to an almost 10^3km [11].

As a preliminary test of our theory, in Figs. 1 and 3 we contrast wavenumber spectra of chlorophyll concentration fields observed in two different regions, the first in which BIG waves dominate the energy spectrum in the given range, and the second where two-dimensional eddy turbulence dominates over all relevant scales. The experimental data analysis approach is described in Appendix B. The first region is at a high latitude of 60°N south of Iceland, and the second at 35°N east of Honshu Island, Japan. The spectral power law in Fig. 3 indeed follows closely the k^{-1} law predicted for eddy induced passive tracer variations [2]. The region for which this spectrum has been estimated is near the Kuroshio current which provides a strong source of 2D eddy turbulence. Fig. 1 displays a much steeper k^{-3} power law behavior consistent with predictions based on BIG waves, equation (41) and the discussion below it. In order to appreciate the relative importance of eddy turbulence as compared to that of BIG wave turbulence, we also analyzed (based on satellite altimeter measurements) the SSH variations in both regions and estimated power spectra of the two basic components contributing to the SSH signal. In Figs. 5 and 5 we show the spectra of the BIG wave component (solid curves) and of the eddy-induced component (dashed curves). Evidently, the relative level of BIG wave turbulence in the high-latitude region, Fig. 5, is much greater than that of eddy turbulence, whereas in the low-latitude region, Fig.5, the opposite is true. As discussed in the Introduction, the dominance of BIG wave turbulence in the high-latitude region of Fig.1 is due to the fact that the energy of eddy turbulence is generated in the high wavenumber range of the spectrum. The chlorophyll concentration field yielding the spectrum in Fig. 3 is shown in Fig. 6.

A Asymptotics of the spectral integral

Consider an integral of the form

$$I(r) = \int \frac{d^d x}{x^{d+\sigma}} e^{-(\mathbf{x}-\mathbf{r})^2/x^\beta}, \tag{48}$$

with σ and β taking any real values. We divide the analysis into several cases.

(i) If $\sigma < 0$ and $\beta < 2$, $I(r)$ remains finite as $r \to 0$, with the former ensuring convergence at small

x and the latter ensuring convergence at large x. On finds then

$$I(0) = \int \frac{d^d x}{x^{d+\sigma}} e^{-x^{2-\beta}} = A_d \Gamma\left(\frac{-\sigma}{2-\beta}\right), \tag{49}$$

where $A_d = 2\pi^{d/2}/\Gamma(d/2)$ is the area of the unit sphere in d dimensions. One may then consider derivatives of $I(r)$ at $r=0$. If $|\sigma|$ is large, the first few of these will in fact be finite. One finds, for example,

$$\begin{aligned} I'(0) &= \int \frac{d^d x}{x^{d+\sigma+\beta-1}} e^{-x^{2-\beta}} \hat{\mathbf{r}} \cdot \hat{\mathbf{x}} = 0 \\ I''(0) &= \int \frac{d^d x}{x^{d+\sigma+\beta}} e^{-x^{2-\beta}} \left[-2 + 4x^{2-\beta}(\hat{\mathbf{r}} \cdot \hat{\mathbf{x}})^2\right] \\ &= -2A_d \Gamma\left(-\frac{\sigma+\beta}{2-\beta}\right) + \frac{4}{d} A_d \Gamma\left(1 - \frac{\sigma+\beta}{2-\beta}\right), \end{aligned} \tag{50}$$

and so on. The most singular term produced by each pair of derivatives effectively decreases $|\sigma|$ by β. This procedure therefore allows the first n Taylor coefficients of $I(r)$ to be computed, where n is the largest integer such that $2|\sigma| - n\beta$ is still positive. The $(n+1)$st derivative produces an integral whose most singular term produces a divergence at $r=0$, i.e. an effective positive value of σ. This case is handled in (iii) below. The result is a subleading, (but leading nonanalytic) contribution to $I(r)$ given exactly by the last line of (51), but with $\sigma < 0$.

(ii) If $\sigma \geq 0$ and $\beta \leq 0$ [which includes the possibility that $\beta = 0$ could correspond to $\ln(1/x)$ behavior], the singularity at small x makes $I(r)$ divergent for all values of r.

(iii) If $\sigma > 0$ and $0 < \beta < 2$, $I(r)$ is finite for any $r > 0$, but diverges as $r \to 0$ due to the singularity at small x. Making the substitution $\mathbf{u} = \mathbf{x}/r^{2/\beta}$ one obtains

$$\begin{aligned} I(r) &= \frac{1}{r^{2\sigma/\beta}} \int \frac{d^d u}{u^{d+\sigma}} e^{-(r^{2/\beta-1}\mathbf{u}-\hat{\mathbf{r}})^2/u^\beta} \\ &= \frac{1}{r^{2\sigma/\beta}} \int \frac{d^d u}{u^{d+\sigma}} e^{-1/u^\beta}[1+o(1)] \\ &= \frac{A_d \Gamma(\sigma/\beta)}{r^{2\sigma/\beta}}[1+o(1)] \end{aligned} \tag{51}$$

where $o(1)$ signifies neglected terms vanishing as $r \to 0$. The condition $\beta < 2$ is required so that $r^{2/\beta-1} \to 0$ as $r \to 0$ in the second line. One requires the inequality $\sigma > 0$ here for convergence at large u. If, pursuant to the discussion in (i), the divergent integral was obtained as the most singular term of the $(n+1)$st derivative of (49) with some initial value $\sigma_0 < 0$ [so that $\sigma = \sigma_0 + (n+1)\beta/2$], then reintegrating (51) $n+1$ times produces a subleading contribution with power law $r^{n+1-2\sigma/\beta} = r^{-2\sigma_0/\beta}$. Using the properties of the Γ function it is elementary to show, as claimed in the last line of (i), that this term then takes exactly the form (51) with σ replaced by σ_0.

(iv) In the special case $\sigma = 0$ and $0 < \beta < 2$, $I(0)$ is still divergent due to the (now logarithmic) singularity at small x. This case is most simply treated by considering the limit $\sigma \to 0^-$. Equation (49) produces $I(0)$, while the leading power law correction can be obtained by examining the derivative

$$\begin{aligned} \frac{dI(r)}{dr} &= -\frac{2}{r^{1+2\sigma/\beta}} \int \frac{d^d u}{u^{d+\sigma+\beta}} e^{-(r^{2/\beta-1}\mathbf{u}-\hat{\mathbf{r}})^2/u^\beta} [1 - \hat{\mathbf{r}} \cdot \mathbf{u} r^{2/\beta-1}] \\ &= -\frac{2}{r} \int \frac{d^d u}{u^{d+\beta}} e^{-1/u^\beta} [1 + o(1)] \\ &= -\frac{2A_d \Gamma(1+\sigma/\beta)}{r^{1+2\sigma/\beta}} [1 + o(1)]. \end{aligned} \tag{52}$$

Integrating this result produces a term in $I(r)$ varying as $r^{-2\sigma/\beta}$. Combining this with $I(0)$ we obtain

$$\begin{aligned} I(r) &= A_d \Gamma\left(\frac{-\sigma}{2-\beta}\right) - A_d \Gamma\left(\frac{\sigma}{\beta}\right) r^{-2\sigma/\beta} \\ &= 2A_d \Gamma(1+\sigma/\beta) \frac{1 - r^{2\sigma/\beta}}{2\sigma/\beta} - \frac{A_d}{\sigma} \left[(2-\beta)\Gamma\left(1 - \frac{\sigma}{2-\beta}\right) - \beta\Gamma\left(1 + \frac{\sigma}{\beta}\right)\right]. \end{aligned} \tag{53}$$

Taking now the limit $\sigma \to 0$, the first term produces a logarithm, while the last term produces the finite result $2A_d\Gamma'(1) = 2A_d\psi(1) = -2A_d C$, where $C = 0.577215\ldots$ is Euler's constant. Thus for $\sigma = 0$ and $0 < \beta < 2$ we finally obtain

$$I(r) = 2A_d[\ln(1/r) - C] + o(1). \tag{54}$$

(v) If $\beta > 2$ the integral defining $I(0)$ is convergent at small x for any value of σ, positive or negative. If $\sigma > 0$ the integral is convergent at large x as well and (49) remains valid. However, if $\sigma \leq 0$ the integral fails to converge at large x. Physically, however, this is an artifact of the power law approximation for $\gamma(x)$, which must saturate to a finite value at $x \simeq \xi$, ξ being the correlation radius of the wave field. With this cutoff, for $\sigma \leq 0$ one finds a strong cutoff dependent $I(0) \sim [1 - \xi^{-\sigma}]/\sigma$ [$\sim \ln(\xi)$ for $\sigma = 0$].

(vi) In the special case $\beta = 2$ the integral defining $I(0)$ is convergent at small x if $\sigma < 0$ but is divergent at large x. One again obtains the cutoff dependent result $I(0) \sim [1 - \xi^{-\sigma}]/\sigma$. Derivatives with respect to r again increase the effective value of σ, and the discussion in (i) is relevant to the extraction of the leading singular term which arises when this effective value first becomes positive. If $\sigma > 0$, $I(0)$ is now convergent at large x but divergent at $x = 0$. The substitution $\mathbf{u} = \mathbf{x}/r$ then yields the *exact* power law form

$$I(r) = \frac{1}{r^\sigma} \int \frac{d^d u}{u^{d+\sigma}} e^{-(\mathbf{u}-\hat{\mathbf{r}})^2/u^2}. \tag{55}$$

Using the result that the angular average of $e^{i\mathbf{k}\cdot\hat{\mathbf{x}}}$ over all directions $\hat{\mathbf{x}}$ is given by

$$\langle e^{i\mathbf{k}\cdot\hat{\mathbf{x}}} \rangle_{\hat{\mathbf{x}}} = \Gamma(d/2)(2/k)^{(d-2)/2} J_{(d-2)/2}(k), \tag{56}$$

we obtain, with $ik \to 1/u$,

$$I(r) = \frac{(2\pi i)^{d/2}}{ier^\sigma} \int_0^\infty \frac{du}{u^{1+\sigma}} u^{(d-2)/2} J_{(d-2)/2}(1/iu) e^{-1/u^2}$$

$$= \frac{\Gamma(\sigma/2)\pi^{d/2}}{e\Gamma(d/2)} {}_1F_1(\sigma/2, d/2, 1/4)\frac{1}{r^\sigma}. \tag{57}$$

where in the last line relation 6.631.1 (p. 716) in [17] has been used. Finally, if $\sigma = 0$, $I(r)$ contains a logarithmic divergence at large x. Applying a cutoff at $x = \xi$, one obtains

$$\begin{aligned} I(r) &= \int_{u<\xi/r} \frac{d^d u}{u^d} e^{-(\mathbf{u}-\hat{\mathbf{r}})^2/u^2} \\ &= A_d \int_1^{\xi/r} \frac{du}{u} + O(1) = A_d \ln(\xi/r) + O(1), \end{aligned} \tag{58}$$

where the $O(1)$ correction depends on the detailed implementation of the cutoff.

Acknowledgement. Part of this work was performed at the Jet Propulsion Laboratory, California Institute of Technology, under contract with the National Aeronautics and Space Administration.

References

[1] Kraichnan, R. H., 1974. *Convection of a passive scalar by a quasi-uniform random straining field.* J. Fluid Mech., **64** (4), 737.

[2] Lesieur, M. and R. Sadourny, 1981, *Satellite-sensed turbulent ocean structure*, Nature **294**, 673.

[3] Mirabel, A. P. and S. A. Monin, 1982, *Physics of Oceans and Atmosphere* **19**, 902.

[4] Gower, J. F. R., K. L. Denman and R. J. Holyer, 1980, *Phytoplankton patchiness indicates the fluctuation spectrum of mesoscale oceanic structure*, Nature **288**, 157.

[5] Deschamps, P. Y., R. Frouin, and L. Wald, 1981, *Satellite determination of the mesoscale variability of the sea surface temperature.* J. Phys. Oceanogr., **11**, 864.

[6] Denman, K. L. and M. R. Abbott, 1994, *Time scales of pattern evolution from cross-spectral analysis of advanced very high resolution radiometer and coastal zone color scanner imagery*, J. Geophys. Res. **99** (C4), 7433.

[7] Charney, J. G., 1971, *Geostrophic turbulence*, J. Atmos. Sci. **28**, 1087.

[8] Eady, E. T., 1949, *Long waves and cyclonic waves*, Tellus **1**(3), 33.

[9] Maltrud, M. E., R. D. Smith, A. J. Semtner, and R. C. Malone, 1998, *Global eddy-resolving ocean simulations driven by 1985-1995 atmospheric winds.* J. Geophys. Res. **103**(C13), 30,825.

[10] Glazman, R. E., 1996, *Spectra of baroclinic inertia-gravity wave turbulence*, J. Phys. Oceanogr. **26**, 1256.

[11] Glazman, R. E. and B. Cheng, 1999, *Altimeter observations of baroclinic oceanic inertia-gravity wave turbulence*, Proc. Roy. Soc. Lond. Ser. A. **455**, 91-123.

[12] Monin, A. S. and A. M. Yaglom, 1971. *Statistical Fluid Mechanics*, Vol.**1**, 769 pp., MIT Press.

[13] Klyatskin, V. I., 1994. *Statistical description of diffusing tracers in random velocity fields*, Physics-Uspekhi bf 37(5), 501.

[14] Herterich, K. and K. Hasselmann, 1982, *The horizontal diffusion of tracers by surface waves*, J. Phys. Oceanogr. **12**(7), 704.

[15] Weichman, P. B. and Glazman, R. E., 1998, *Passive scalar transport by travelling wave fields* (preprint).

[16] Piterbarg, L. I., 1997, *Short-correlation approximation in models of turbulent diffusion* in: "Stochastic Models in Geosystems" (Springer, New York), S. A. Molchanov and W. A. Wojczinski, editors), p. 313.

[17] I. S. Gradshteyn and I. M. Rhyzhik, 1981, *Table of Integrals, Series, and Products* (Academic Press, New York).

Figure 1: Power spectrum of chlorophyll-a fluctuations in a 180km×250km ocean area south of Iceland, as reported in Ref. [4] based on analysis of the Landsat multispectral imagery: triangles represent the experimental data, the dashed line is a $k^{-2.92}$ power law found as a least-square fit to the data. [Reproduced courtesy of the authors].

Figure 2: Theoretical spectrum of sea surface height variations [proportional to the potential energy spectrum, $U(k)$], dominated by the inverse cascade of BIG wave energy. The computation is based on that in Ref. [10], with an assumed geographic latitude of 20°.

Figure 3: Power spectrum of chlorophyll-a fluctuations in an ocean area east of Honshu Island (Japan), based on analysis of the OCTS multispectral imagery obtained from the ADEOS satellite (courtesy of the Japanese Space Agency NASDA). Dashed line: power law k^{-1} for comparison.

Figure 4: Power spectra of sea surface height fluctuations in a region south of Iceland. Based on analysis of Topex/Poseidon ocean altimeter measurements [Glazman and Cheng, 1999]. Solid curve represents the component of the total SSH spectrum associated with the vortical motions. Dashed curve represents the component caused by the (much faster) gravity-wave motions. Both spectra are proportional to the potential energy of the corresponding type motions. Dotted line ($k^{-11/3}$) corresponds to the Kolmogorov $k^{-5/3}$ law for the inverse cascade of energy through the spectrum of 2D eddy turbulence.

Figure 5: Power spectra of sea surface height fluctuations in a region east of Honshu Island, Japan. Solid and dashed curves are as in Fig. 5. The dotted curve (k^{-5}) corresponds to the Kraichnan k^{-3} law for the direct cascade of enstrophy through the spectrum of 2D eddy turbulence.

Figure 6: Chlorophyll-a field corresponding to Figs. 3 and 5.

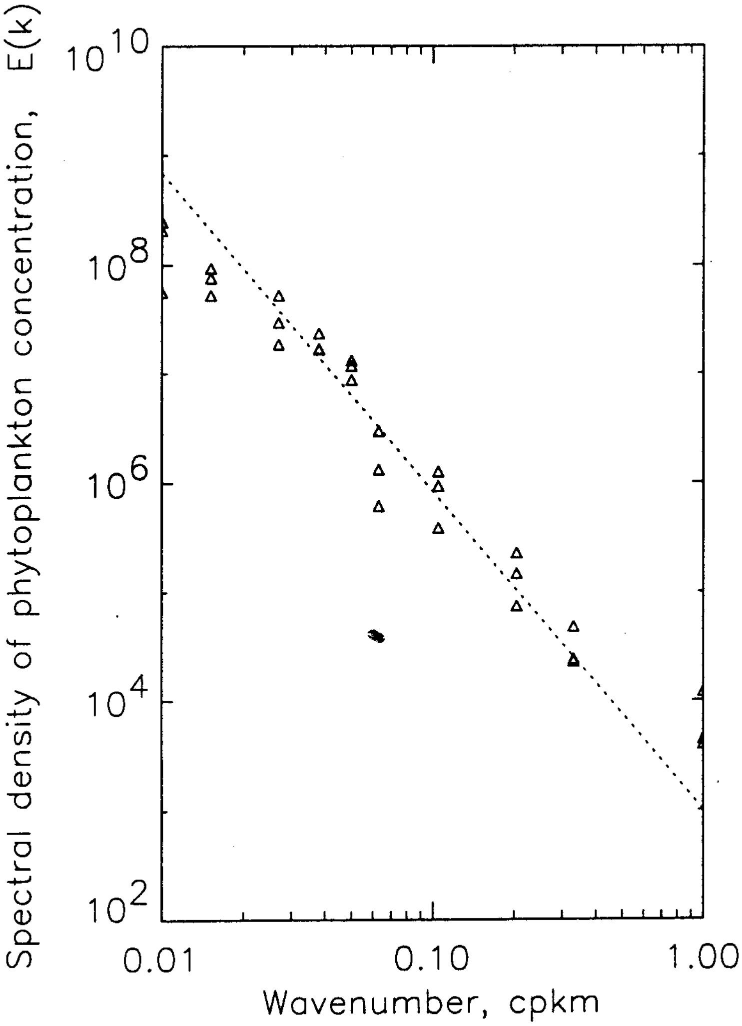

Spectral density of phytoplankton concentration, E(k)
10^{10}
10^{8}
10^{6}
10^{4}
10^{2}
0.01
0.10
1.00
Wavenumber, cpkm

Fig. 1

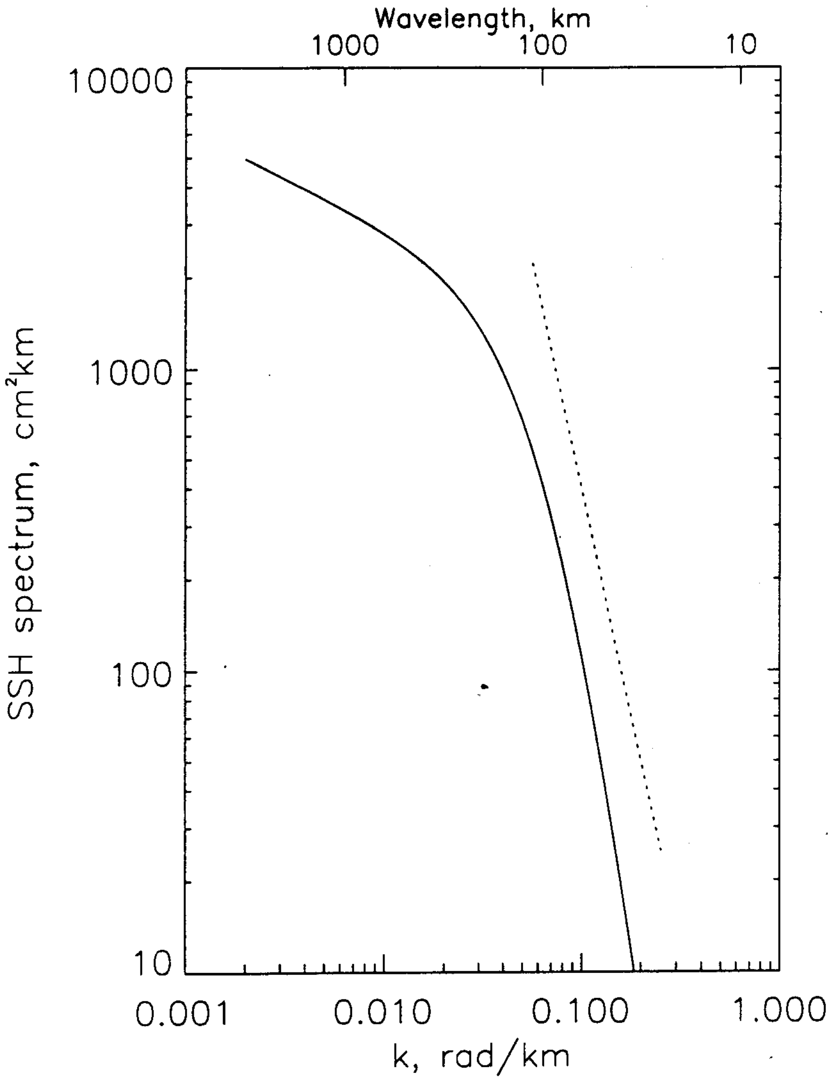
Wavelength, km
1000
100
10
10000
1000
100
10
SSH spectrum, cm²km
0.001
0.010
0.100
1.000
k, rad/km

Fig. 2

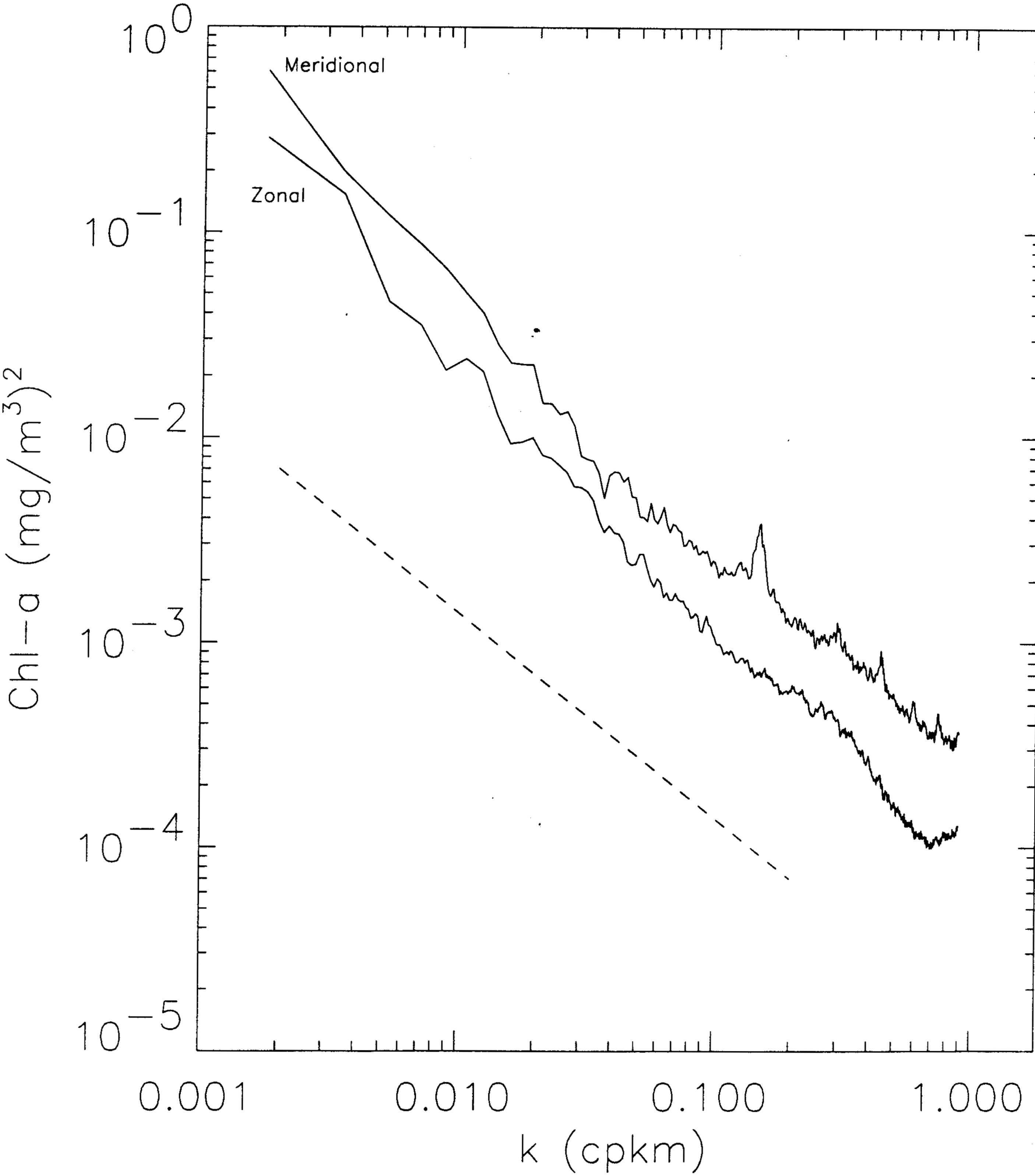
Meridional
Zonal
10^0
10^{-1}
10^{-2}
10^{-3}
10^{-4}
10^{-5}
Chl-a $(mg/m^3)^2$
0.001
0.010
0.100
1.000
k (cpkm)

Fig 3

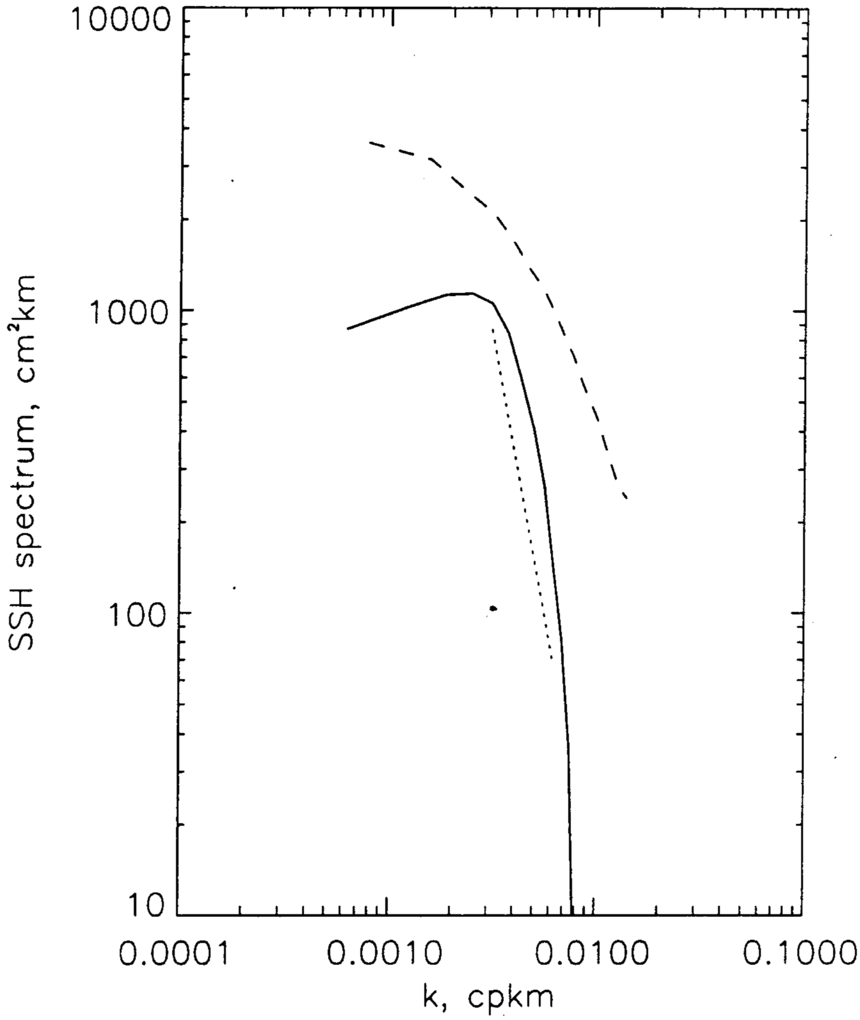

10000
1000
100
10
SSH spectrum, cm²km
0.0001
0.0010
0.0100
0.1000
k, cpkm

Fig. 4

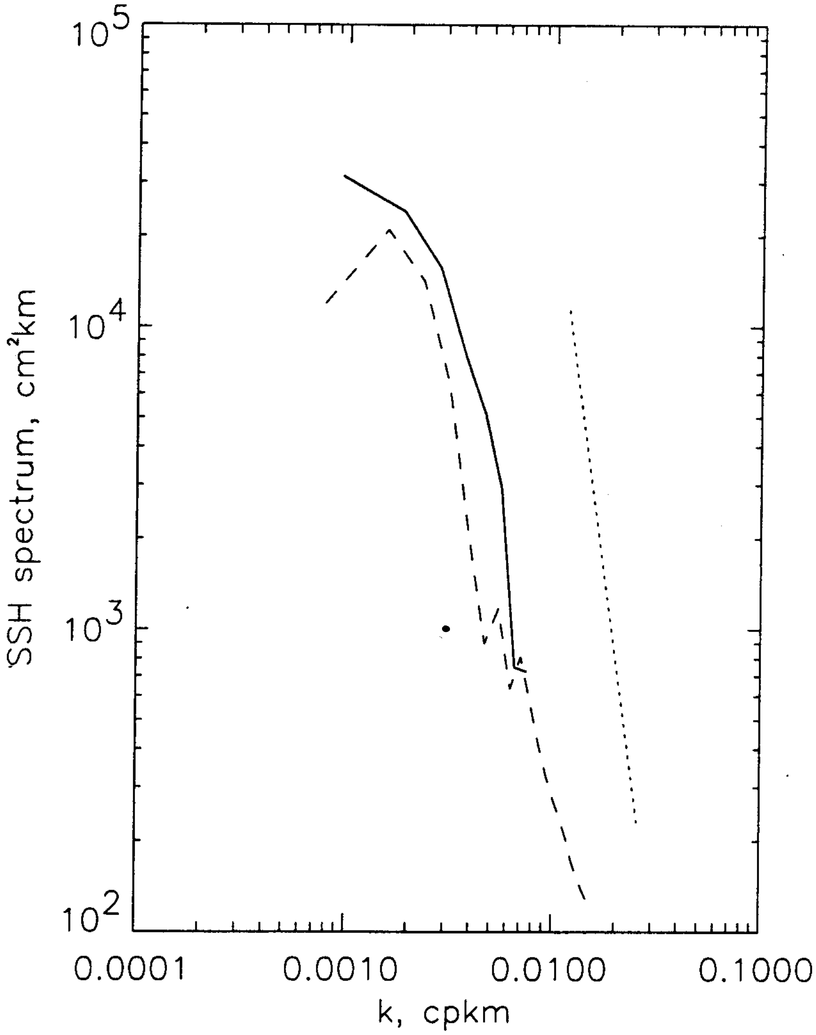

10^5
10^4
10^3
10^2
SSH spectrum, cm²km
0.0001
0.0010
0.0100
0.1000
k, cpkm

Fig. 5